Glyphosate retention dynamics at organo-mineral interfaces: Formation of multiple hydrogen-bonds and inner-sphere configurations at pectin-goethite interfaces

Behrooz Azimzadeh and Carmen Enid Martínez*

Soil and Crop Sciences, School of Integrative Plant Science, College of Agriculture and Life Sciences, Cornell University, Ithaca, New York 14853, USA

Keywords

glyphosate, pectin, goethite, organo-organic interactions, organo-mineral association, adsorption-desorption kinetics, *in-situ* ATR-FTIR, hydrogen bonding

Abstract

The retention of glyphosate is strongly governed by adsorption and desorption processes at environmental interfaces. In particular, glyphosate can react with organo-mineral associations (OMAs) in soils, sediments, and aquatic environments. Here, we use *in-situ* time-resolved attenuated total reflectance Fourier-transform infrared (ATR-FTIR) spectroscopy to provide a mechanistic understanding of glyphosate's adsorption and desorption processes at an organo-mineral interface. Pectin-goethite complexes prepared with a range of pectin concentrations $(0.25 - 4.0 \text{ mg mL}^{-1})$ were used as model OMAs with varying organic surface loading. Adsorption and desorption kinetic studies were conducted by sequentially introducing a 4.0 mM glyphosate solution and a 10 mM KCl solution, respectively, over pectin-goethite films until equilibrium was reached. All experiments were conducted at pH = 5.0. ATR-FTIR spectra reveal adsorbed-pectin significantly alters the rate, quantity and binding mechanisms of glyphosate in pectin-goethite compared to goethite films. Our results illustrate, for the first time, that multiple hydrogen bonds between oxygen- and nitrogen- containing residues of adsorbed-pectin and glyphosate enhanced the relative retention of glyphosate at pectin-goethite interfaces and decreased desorption. It is also observed that glyphosate's phosphonate moiety preferentially forms inner-sphere mononuclear complexes with goethite in pectin-goethite films whereas binuclear configurations are more favorable in goethite films. Since the proportion of organo-mineral to mineral interfaces decreases with soil depth, this work provides insights as to the extent, kinetics and mechanisms that might be involved during glyphosate downward transport in soils. Overall, our findings have valuable implications for characterizing and predicting the fate and behavior of glyphosate at heterogeneous interfaces present in natural systems.

Introduction

When surface-applied to agricultural land, side roads, and individuals' home gardens and lawns, glyphosate (*N*-(phosphonomethyl)glycine) interacts with mineral and organic-coated mineral surfaces potentially affecting its mobility and efficiency as an herbicide. Since the mobility and distribution of herbicides in soil is generally mediated by water transport, adsorption-desorption processes at these interfaces are deemed important. Glyphosate is the world's most heavily applied herbicide[1] and its use has raised concerns about its effects on the environment[5] and on human health. [2-4]

Glyphosate is a polar organic molecule and a zwitterion at relevant environmental conditions, with a tridentate character due to its amino, carboxylic, and phosphonic functional groups.[5, 6] A large number of studies show that glyphosate can strongly interact with metal ions in solution and at water-mineral interfaces,[4, 5, 7-10] particularly with iron (hydr)oxides through its phosphonic group.[7-9, 11-15] The role of organic-coated mineral surfaces (i.e., organo-mineral associations, OMAs) on the mobility and distribution of glyphosate in soils is far less studied and understood. A few studies have shown that OMAs may inhibit, retard or enhance the mobility of glyphosate in the environment.[12, 16] For example, humic acid-goethite associations have been shown to increase glyphosate mobility, presumably a result of electrostatic repulsion due to the negative charge conferred by sorbed humic acid and by a reduction in the availability of active mineral surface sites.[12] Conversely, a more recent study [16] demonstrated that a humic acid-kaolinite association can adsorb higher amounts of glyphosate than kaolinite alone. In the latter study, the authors suggested a ternary adsorption system in which glyphosate binds to the interfacial hydroxyl groups in humic acid-kaolinite associations via hydrogen bonds involving carboxyl, amino, and phosphonyl moieties of glyphosate. It is clear we are unable to conceptualize or

predict the effect OMAs might have on glyphosate retention. In addition, previous studies have failed to consider desorption dynamics when assessing glyphosate behavior at these heterogeneous organo-mineral interfaces.

Here, we present a series of molecular-scale, time-resolved, and surface-sensitive sorption-desorption studies using goethite and pectin-goethite associations as model interfaces. Goethite, an iron (hydr)oxide (α-FeOOH), is used as a model mineral in experiments since it is commonly present in soils and frequently used in glyphosate sorption studies.[9, 12, 14, 17-20] We chose pectin, a naturally occurring macromolecule present in plant cell walls, as a model organic molecule present in OMAs. Pectin is ubiquitously present in soils and potentially acts as a binding agent in the soil matrix.[21, 22] The structure of pectin is well-known: a linear polysaccharide composed of α-1,4-linked galacturonic acid units. The polymer is methyl esterified to various degrees and it contains amide functional groups.[23, 24]

In this study, we determine the kinetics and mechanisms of interaction of glyphosate at the goethite and pectin-goethite interfaces and aim to investigate the effect increasing pectin surface loading might have on these interactions. Experimentally, we use *in-situ* time-resolved ATR-FTIR spectroscopy to obtain adsorption-desorption kinetic parameters and to decipher its mechanisms of interaction. The capabilities of ATR-FTIR to obtain kinetic information of environmentally relevant systems has been demonstrated in several studies.[12, 25, 26] Furthermore, ATR-FTIR analyses permit the identification of glyphosate's interfacial species in different bonding environments and the functional groups involved in such interactions. We focus on deciphering the contribution of each functional group of the glyphosate molecule (amino, carboxylate, phosphonate) to its interaction with goethite and pectin-goethite associations during adsorption and desorption processes. To our knowledge, this is the first study highlighting

glyphosate's adsorption-desorption dynamics at organo-mineral interfaces at the molecular-scale, in solution and in real time. These studies provide new molecular-scale knowledge that further our understanding of glyphosate's sorption-desorption dynamics at heterogeneous organo-mineral interfaces.

Materials and Methods

Materials

Glyphosate (96 % purity) was purchased from Sigma-Aldrich (Milwaukee, USA). Pectin from citrus fruit (Sigma-Aldrich, Prod. No. P9436) was used in experiments as received without further purification. This product has a MW of ≈ 71.1 kDa,[27-29] and a $pK_{a(COOH)} = 3.3 - 4.5$.[30] All solutions and suspensions were made with deionized water (18.2 MΩ resistance), boiled and purged with N_2 gas to remove dissolved CO_2. In all experiments, a 10 mM KCl background electrolyte was used to approximate the low ionic strength of soil solutions.

Goethite used in experiments was synthesized by the method of Schwertmann and Cornell.[31] Details of mineral synthesis can be found in the Supplementary Information (SI, S1). Identity and purity of the synthesized goethite was verified with FTIR (Figure S1). The surface area and particle size were determined to be 44.2 ± 2.9 m^2 g^{-1} and 32.0 ± 2.1 by N_2 adsorption with an ASAP2460 instrument (Micromeritics Instrument Corp.) respectively. pH at the point of zero charge (pH_{pzc}) value of the synthesized goethite obtained by salt titration approach[32, 33] was 7.3 ± 0.2 (Figure S2).

FTIR Instrument Parameters

ATR-FTIR (attenuated total reflectance Fourier-transform infrared) spectra were collected on a Vertex 70™ FTIR spectrometer (Bruker Corp., Billerica, MA) equipped with a deuterated L-alanine-doped triglycine sulfate detector. A Pike GladiATR™ accessory with a single-bounce diamond internal reflection element (IRE) and flow cell (Pike Technologies Madison, WI) was used for sampling. Atmospheric stability of the instrument and sample compartments was attained by continuous purging with dry air. Spectra representing an average of 200 scans were collected from 4500 to 150 cm^{-1} with a spectral resolution of 4 cm^{-1}. After collection, spectra received an atmospheric compensation, a nine-point Savitsky-Golay smoothing and baseline correction to remove instrumental drift. All post-hoc manipulations were performed using OPUS v.7.2 software (Bruker Corp., Billerica, MA).

In-situ time-resolved ATR-FTIR Experiments

The workflow of *in-situ* ATR-FTIR experiments (Figure S3) and methodological details are reported in the SI (S2). Goethite films used in experiments were produced by drop casting 4.8 μL of a 1.68 g L^{-1} suspension of goethite over the diamond IRE and drying under N_2 flow. Upon deposition, 10 mM KCl background solution was passed over the goethite film at a rate of 0.9 ± 0.05 mL min^{-1} to remove any loosely bound material and allow for rehydration of the film. Film stabilization was conducted until no detectable changes to the FTIR spectrum were observed ($\approx$ 120 min). At this point, a background spectrum was collected. Formation of pectin-goethite organo-mineral associations (OMAs) was initiated by exchanging the background solution with a pectin solution. A range of surface loadings were obtained by passing different initial concentrations of pectin ([Pt] = 0, 0.25, 0.50, 1.00, 2.00, 3.00, and 4.00 mg mL^{-1}) over goethite films for a fixed time ($\approx$ 180 min). Adsorbed pectin was stabilized by passing the same

background electrolyte (10 mM KCl) at a rate of 0.85 ± 0.05 mL min^{-1} to remove any loosely

bound pectin. Stability of pectin-goethite OMAs was considered to be attained when no changes

were observed in interfacial spectra collected during background solution flow (≈ 60 min). At

this point, a new background spectrum was collected, and adsorption of glyphosate was initiated

by exchanging the background solution with a fixed 4 mM glyphosate solution at a rate of $0.85 \pm$

0.05 mL min^{-1} until equilibrium (≈ 86 min). Glyphosate adsorption was followed by a desorption

step using the same background solution and rate, until equilibrium (≈ 72 min). Solutions with a

pH of 5.0 were used for all experiments, which represent environmentally relevant conditions.

The pH was maintained within 0.05 pH units throughout experiments by regulated additions of

0.005 M HCl or KOH with a pH controller. To determine the uncertainty in our measurements,

experiments were repeated 4 times on freshly prepared films under identical conditions. All

ATR-FTIR experiments were conducted under ambient atmosphere. Solution spectra of

glyphosate and pectin were collected at concentrations of 0.10 M and 8.00 mg mL^{-1},

respectively, in a 10 mM KCl background solution at pH = 5.0. All spectra were collected by

subtracting the spectrum of the background electrolyte from the spectrum of each sample. In this

way, the difference spectrum contains only the absorption bands of interfacial species, including

inner- and outer- sphere species and bands of "free" or uncomplexed species in the bulk solution.

ATR-FTIR Data Processing

Two regions of the ATR spectra, namely, the phosphonate frequency region ($1100 - 950$ cm^{-1})

and the carboxylate-amine frequency region ($1700 - 1500$ cm^{-1}) were cut and further processed.

The integral of the baseline-corrected IR peaks of the phosphonate region was used to probe total

glyphosate adsorption and desorption kinetics and P-O band coordination to Fe(III). The spectral

features in the 1700-1500 cm^{-1} range were deconvoluted in order to determine potential hydrogen bonding and the contribution of carboxylate (v_{as}(COO$^-$)) and amine (δ(NH$_2^+$)) moieties in interfacial complex formation and subsequent dynamicity of adsorbed glyphosate. After cutting and baseline correction, peak fitting of the spectra was carried out using a second derivative deconvolution algorithm and subsequent Gaussian curve fitting to identify and quantify spectral features corresponding to $\underline{v_{as}}$(COO$^-$) and δ(NH$_2^+$) vibrational modes. The second derivative of spectra was calculated with minima aligning with component peak maxima positions. Identified peak maxima position values were used as input parameters and fixed for fitting. Gaussian peak full width at half-maximum and peak height were allowed to float throughout fitting. The Levenberg-Marquardt algorithm was used to optimize the fitting of Gaussian curves to experimental data. Calculation of second derivative spectra and curve fitting were performed using Peakfit v.4.12 software (Systat Software Inc., San Jose, CA).

Adsorption-desorption Kinetic Models

Integral of FTIR bands ($A(\tilde{v_i})$) of glyphosate during adsorption and desorption steps were fitted with two commonly used kinetic models, the Lagergren's pseudo-second-order (PSO) and pseudo-first-order (PFO) models, respectively. The PSO model for adsorption processes can be described by the following equation:[34]

$$A(\tilde{v_i})_{t,ads} = \frac{k_{2,ads} A(\tilde{v_i})_{e,ads}^2 t}{1 + k_{2,ads} A(\tilde{v_i})_{e,ads} t} \qquad (Eq.\ 1)$$

where $A(\tilde{v_i})_{t,ads}$ is the integral absorption intensity of the glyphosate band(s) (a.u.) at adsorption time t (min), $k_{2,ads}$ is the PSO rate constant (min^{-1} a.u.$^{-1}$), and $A(\tilde{v_i})_{e,ads}$ is the integral absorption intensity of the glyphosate band(s) at equilibrium (a.u.).

Desorption of glyphosate was described by a modified PFO model represented by the following equation:[26]

$$A(\tilde{v}_i)_{t,des} = (\alpha - A(\tilde{v}_i)_{e,des})e^{-k_{1,des}t} + \alpha \qquad \text{(Eq. 2)}$$

where $A(\tilde{v}_i)_{t,des}$ is the integral absorption intensity of the glyphosate bands (a.u.) at desorption time t (min), $k_{1,des}$ is the PFO rate constant (min^{-1}), $A(\tilde{v}_i)_{e,des}$ is the integral absorption intensity of the glyphosate bands at desorption equilibrium (a.u.), and α is a dimensionless constant that locates the desorption curve that follows just after the adsorption curve at equilibrium. Empirically, ln(α) is directly proportional to $A(\tilde{v}_i)_{e,ads}$ and to the adsorption-desorption process. The PFO model was also applied to describe pectin's adsorption and desorption kinetics at the goethite interface during formation and stabilization of pectin-goethite OMAs (SI). All fitting was completed with the nonlinear curve fitting GraphPad Prism v.6.02 software.

Results and Discussion

Pectin and Goethite Form Organo-mineral Associations.

A series of pectin-goethite OMAs were prepared with varying pectin surface loading for our study. Figure 1A shows a representative set of *in-situ* time-resolved ATR-FTIR spectra collected during pectin's coating (i.e., adsorption) and stabilization (i.e., desorption) over a goethite film. Corresponding peak assignments are shown in Table S1. Interfacial spectra indicate the progression of pectin adsorption through increasing signals of skeletal bands of the pyranose rings (e.g., $v(CC)(CO)_{ring}$) and α-1,4 glycosidic bonds (e.g., $v_{as}(COC)_g$) from 1200 – 950 cm^{-1}.[35-37] Intense peaks within the 1780 – 1200 cm^{-1} range are also observed and are assigned to different band types of residual groups in the galacturonic acid rings.[24, 30, 37-42] In a recent work,

we tentatively relate these bands to different interfacial interactions that govern pectin adsorption at the goethite surface, including electrostatic attraction with the goethite surface and multiple hydrogen-bonding interactions within adsorbed pectin chains.[43] In addition, adsorption of pectin onto goethite appears to be coupled to dehydration at the surface.[43]
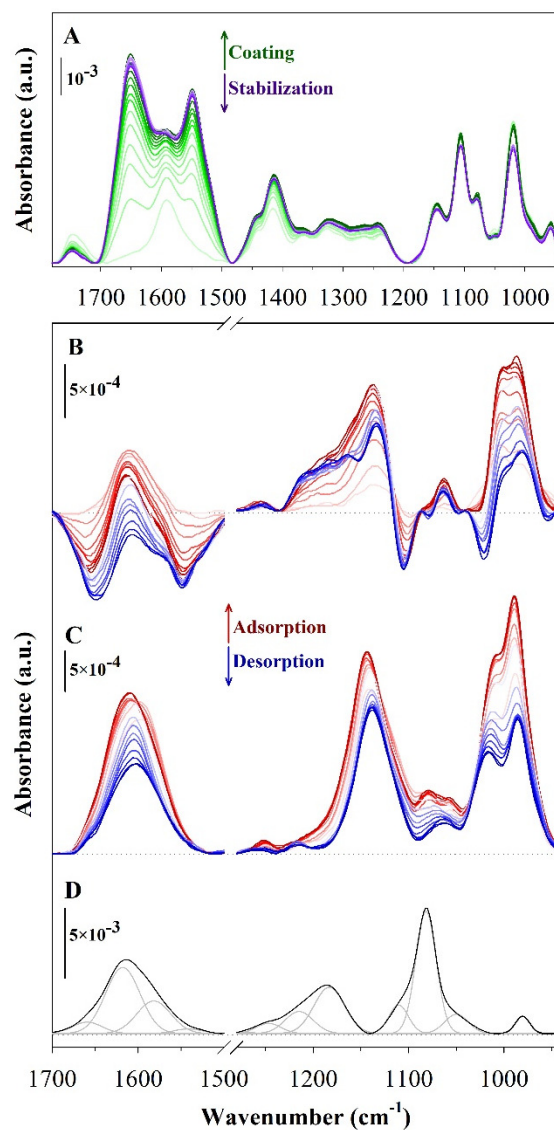

Figure 1. Representative baseline corrected ATR-FTIR spectra in the 1780 – 940 cm^{-1} range. (A) Spectra highlight the formation (coating) and stabilization of pectin-goethite OMAs (2.0 mg mL^{-1} pectin on goethite). Glyphosate's (4 mM) adsorption-desorption dynamics at the (B) pectin-goethite and (C) goethite interface. Red and blue lines in (B) and (C) indicate the evolution of

interfacial spectra collected every ≈ 8 minutes during glyphosate adsorption-desorption experiments, respectively. (D) ATR-FTIR spectrum for glyphosate (0.10 M) in 10 mM KCl supporting electrolyte solution at pH 5.0. Gray lines show deconvoluted ATR-FTIR components of glyphosate using the second derivative method. Note spectra in (B), (C) and (D) are truncated to highlight the carboxylate-amine ($v(CAc)$, 1700 – 1500 cm^{-1}) and phosphonate ($v(PO)$, 1250 – 950 cm^{-1}) regions of the spectra.

Kinetic data (Figure 2A), monitored using the $v(CO)(CC)_{ring}$ peak height backbone vibration of pectin centered at 1106 cm^{-1} (Figure 1A, Table S1), indicates stable OMAs formed between pectin and goethite with only a small fraction of adsorbed pectin removed from the surface at the end of the stabilization phase (4.8 – 9.6%, Table S2). The kinetics of pectin coating formation (i.e., adsorption or phase 1) and stabilization (i.e., desorption or phase 2) are well described by a PFO model (Figure 2A, Table S2). Estimated $k_{1,ads}$ and $k_{1,des}$ values indicate pectin coating formation and stabilization become faster with increasing pectin concentration. Pectin coating formation and stabilization on goethite is well described by the Langmuir isotherm (Figure 2B, Table S3), yielding equilibrium binding constants, K_L, of 6.38 and 7.52 × 10^5 M^{-1} (respectively), while surface saturation is approached at [Pt] > 1.00 mg mL^{-1} (Figure 2B). These K_L values are similar to those reported for protein adsorption on montmorillonite (K_L = 8.7 – 5.97 × 10^5 M^{-1})[44] but much lower than those reported for DNA adsorption on goethite (K_L = 3.2 × 10^8 M^{-1})[45] using the same approach (*In-situ* ATR-FTIR). Pectin surface saturation (A_∞) was reduced by 12.5 % upon the introduction of glyphosate in adsorption-desorption experiments at the stabilized pectin-goethite interface (Figure 2B, Table S3). The observed decrease in pectin's surface saturation is accompanied by a decrease in the equilibrium binding constant (K_L = 4.8 × 10^5 M^{-1}),

suggesting that glyphosate, and potentially other low molecular weight organics, might have a destabilizing effect on OMAs present in soils.[46, 47]
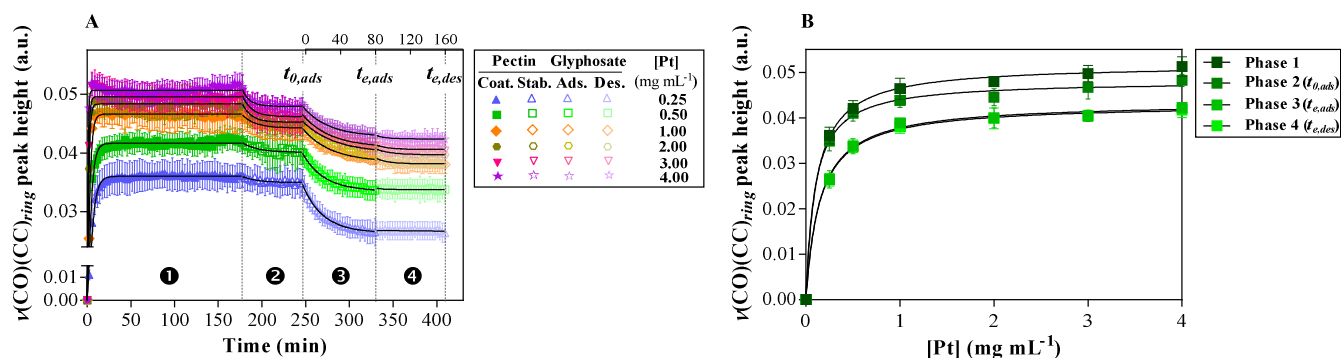

Figure 2. Formation and stability of pectin-goethite OMAs. (A) Evolution of $v(CO)(CC)_{ring}$ vibrations (1106 cm^{-1}) in kinetic experiments during coating (phase 1) and stabilization (phase 2) of pectin-goethite OMAs. Also shown is the evolution of $v(CO)(CC)_{ring}$ vibrations during glyphosate (4.0 mM) adsorption (phase 3) and desorption (phase 4) steps, where $t_{0,ads}$ = time of initial glyphosate addition to stable pectin-goethite OMAs, $t_{e,ads}$ = time for glyphosate adsorption equilibrium and $t_{e,des}$ = time for glyphosate desorption equilibrium. Black lines represent PFO kinetic fits. (B) Sorption isotherms for pectin on goethite at experimental phases 1-4. Black lines indicate Langmuir isotherm models. Error bars represent standard deviation values from replicates (n = 4).

Glyphosate Retention at the Goethite and Pectin-goethite Interface

With reported acid dissociation constants of pK_{a2} = 2.3 (carboxylic), pK_{a3} = 5.5 (phosphonic) and pK_{a4} = 11.0 (amine),[18, 48, 49] the predominant species of glyphosate at pH 5.0 and I = 10 mM is the monoanion [$^-$OOCCH$_2$N$^+$H$_2$CH$_2$-HPO$_3^-$] (69.78 %), with lesser contributions from its

dianion [$^-$OOCCH$_2$N$^+$H$_2$CH$_2$-PO$_3$$^{2-}$] (30.09 %) and trianion [$^-$OOCCH$_2$NHCH$_2$-PO$_3$$^{2-}$] (0.13 %)

species. Based on the deconvoluted ATR-FTIR spectrum of a glyphosate solution (Figure 1D)

and associated peak assignments (Table S4), the characteristic vibrational modes of the

carboxylate group, including v_{as}(COO$^-$) and v_s(COO$^-$) are observed at 1618 and 1403 cm^{-1} (not

shown), respectively,[7-9] while an additional weak vibration is present at 1660 cm^{-1}. The identified

bands at 1581 and 1542 cm^{-1} are tentatively attributed to deformation modes of the amine group,

which occur within the same vibrational envelope as the v_{as}(COO$^-$) vibrational modes.[7-9] The

prominent peaks at 1181 and 1080 are assigned to v_{as}(PO$_2$) and v_s(PO$_2$) in R-HPO$_3$$^-$,

respectively,[4, 7-9, 50] whereas the peak at 978 cm^{-1} is attributed to v(PO$_3$) in R-PO$_3$$^{2-}$.[6-8, 51] The

extent and nature of the interactions between glyphosate and goethite and between glyphosate

and pectin-goethite OMAs were analyzed based on the magnitude and induced shifts in ATR-

FTIR frequencies during adsorption-desorption experiments.

Representative ATR-FTIR spectra of glyphosate's retention dynamics at the pectin-goethite

and goethite interface highlight the progression of glyphosate adsorption and desorption through

increases and decreases in intensity of the phosphonate, carboxylate, and amine bands of the

spectra (Figure 1B-C). Phosphonate (v(PO), 1050 – 950 cm^{-1}) and carboxylate-amine (v(CAc),

1700 – 1500 cm^{-1}) integrated band areas are a measure of glyphosate's surface-associated

species.[8, 12] Vibrational modes within the v(PO) band area include inner-sphere (*IS*) (e.g., P-(O-

Fe)$_{2-n}$) and outer-sphere (*OS*) species (e.g., (PO$_3$)$_{OS}$ or (PO$_2$)$_{OS}$) (Table S4).[8, 9, 12, 14] It is clear

from Figure 1B-C that the proportion and type of inner- and outer-sphere phosphonate-associated

species in pectin-goethite differ from that in goethite. The involvement of glyphosate's

carboxylate and amine functional groups in binding is also apparent in spectra (Figure 1B-C).

The carboxylate-amine v(CAc) integrated band area, which includes surface-associated v(COO$^-$)

and $\delta(NH_2^+)$ vibrational modes (Table S4),[7, 8, 20] is diminished in intensity upon glyphosate interaction with pectin-goethite compared to goethite (Figure 3B). Furthermore, $\delta(NH_2^+)$ contributions to the overall $v(CAc)$ band area seem to increase in pectin-goethite. Although negative FTIR peaks in humic acid-goethite OMAs have been attributed to decreases in glyphosate retention,[12, 19, 52] we attribute the negative progressive peaks in pectin-goethite ATR-FTIR spectra (at least partially) to desorption of pectin from OMAs upon glyphosate adsorption (Figure 2B). Overall, however, spectra indicate sorbed pectin reduced glyphosate retention (Figures 1B-C and 3A-B). As discussed below, pectin-goethite OMAs also had a profound impact on the kinetics and mechanisms of interaction of glyphosate at these heterogeneous interfaces.

Influence of Pectin on Glyphosate Retention: Adsorption-desorption Kinetics and Contribution of Phosphonate, Carboxylate and Amine Functionalities.

Increased pectin loading in pectin-goethite OMAs impacts glyphosate's adsorption-desorption kinetics and the contribution of observed surface-associated bands (Figure 3, Table S5, Figure S4). We found adsorption of glyphosate was impeded as the pectin loading increased in pectin-goethite associations (Figures 3A-B and S4A). This is in good agreement with Arroyave *et al.*[12], where glyphosate adsorption to humic acid-goethite associations was hindered, but it is contrary to the results of Guo *et al.*[16] where higher amounts of glyphosate were adsorbed onto humic acid-kaolinite associations. Variability in the results might be linked to the stability of the organo-mineral association, where humic acid and pectin bind strongly onto goethite whereas weak interactions dominate in humic acid-kaolinite associations. Adsorption-desorption kinetics for $v(PO)$ were described by the PSO and PFO kinetic models, respectively (Table S5). The $v(PO)$-

associated adsorption rate constants ($k_{2,(PO)ads}$) decreased in the presence of 0.25 mg mL^{-1} pectin (Figures 3A and S4B, Table S5) although higher pectin loadings did not seem to have an effect. These results suggest access of the phosphonate group of glyphosate for the active sites on goethite was diminished by the primary layer of pectin and further accumulation of pectin was less effective in reducing phosphonate interactions at the goethite surface. The steady decrease observed in the desorption rate constants ($k_{1,(PO)des}$) and integral absorption intensity ($A_{e,(PO)des}$) of $v(PO)$, that stabilizes at [Pt] $\geq$ 2 mg mL^{-1}, suggest the presumed thicker pectin layers slow down desorption of $v(PO)$'s outer-sphere (OS) species. Similar adsorption behavior has been reported in humic acid-goethite systems, however, these studies did not include a desorption phase.[12]

As demonstrated in Figure 3B, the intensity of $v(CAc)$-associated bands was substantially diminished at the lowest pectin surface loading ([Pt] = 0.25 mg mL^{-1}). Like for $v(PO)$, $v(CAc)$ adsorption-desorption kinetics were described by the PSO and PFO kinetic models, respectively. Estimated adsorption rate constants of $v(CAc)$ ($k_{2,(CAc)ads}$) in Table S5 and Figure S4B indicate the addition of $v(CAc)$ bands becomes slower with increasing pectin surface loading on pectin-goethite. The lowest rates were obtained at [Pt] $\geq$ 2.0 mg mL^{-1}. Estimated values of $k_{2,(PO)ads}$ and $k_{2,(CAc)ads}$ indicate carboxylate-amine moieties of glyphosate interact with faster kinetics compared to phosphonate moieties at [Pt] < 2.0 mg mL^{-1}. The fact that different IR bands of the same compound (i.e., glyphosate) evolve at different rates indicates the presence of more than one adsorbed species.[53] This non-alignment in adsorption kinetic behavior of $v(PO)$ and $v(CAc)$ may be related to distinct contributions of IS and OS interactions of surface-associated glyphosate molecules at the goethite and pectin-goethite interfaces. Still, desorption rate constants ($k_{1,(PO)des}$ and $k_{1,(CAc)des}$) show similar kinetic trends with the carboxylate-amine moiety presenting appreciably slower desorption rates (Figure S4).
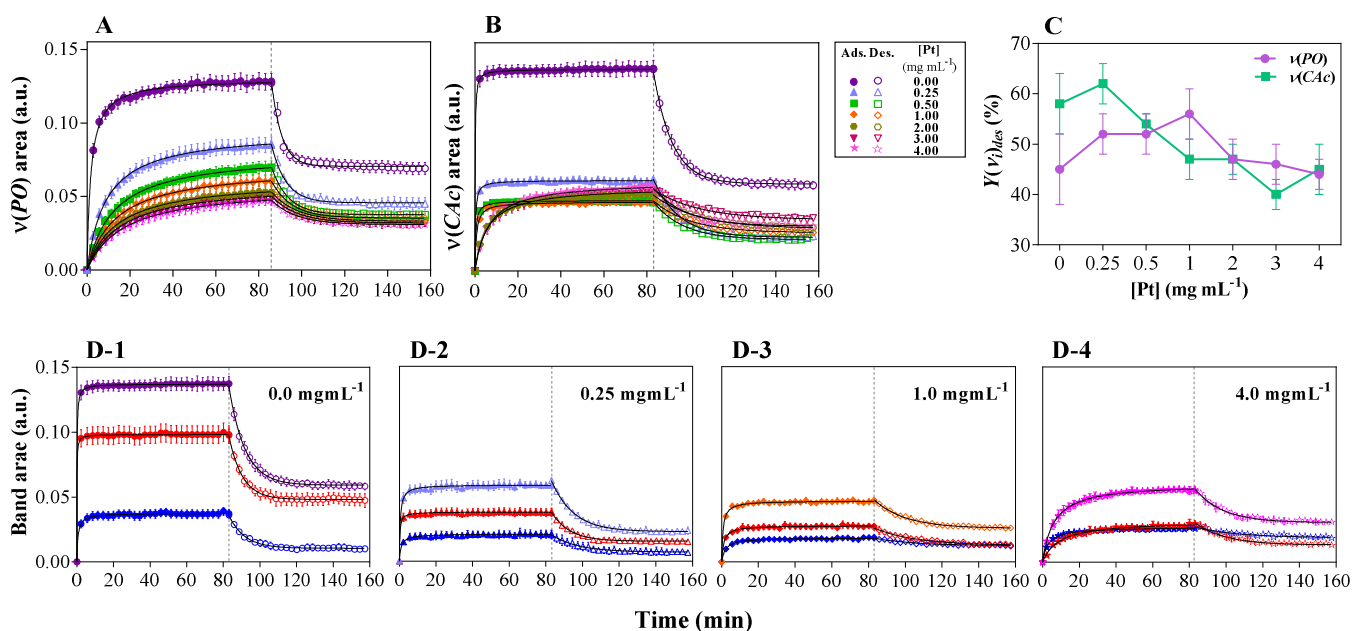
Figure 3. Glyphosate adsorption-desorption kinetics of observed integrated (A) phosphonate ($v(PO)$, $1100 – 950$ cm^{-1}) and (B) carboxylate-amine ($v(CAc)$, $1700 – 1500$ cm^{-1}) bands with increased pectin surface loading. (C) shows the removed fraction ($Y_{(vi)des}$) of $v(CAc)$ and $v(PO)$ at desorption equilibrium. D-1 to D-4 indicate deconvoluted components of $v(CAc)$ at pectin concentrations of 0, 0.25, 1.0, and 4.0 mg mL^{-1}. Red and blue symbols in D represent integrated $v_{as}(COO^-)$ and $\delta(NH_2^+)$ bands, respectively. Also shown in D-1 to D-4 are the integrated $v(CAc)$ band areas with color of symbols corresponding with those in (B). Black lines represent PSO and PFO kinetic fits for adsorption-desorption series, respectively. Dashed vertical lines split glyphosate's adsorption and desorption phases.

Moreover, the relative fraction of $v(CAc)$ removed from the surface at desorption equilibrium ($Y_{(CAc)des}$), and its corresponding desorption rates, were higher at the lowest (0.25 and 0.50 mg

16

mL^{-1}) pectin surface loadings (Figures 3C and S4B, Table S5). Although no clear trend is observed for $Y_{(PO)des}$, the rate of removal was faster for $v(PO)$ across all pectin surface loadings compared to that of $v(CAc)$ (Figure S4B). These results may partly support previous findings that the carboxylate and amine moieties of glyphosate predominantly participate in *OS* complexes compared to $v(PO)$ that mainly form *IS*-associated species.[8, 9, 12, 14] Since increasing pectin surface loading results in less $v(CAc)$ removed from the surface at a slower rate, we suggest that glyphosate's retention at pectin-goethite interfaces is likely more favorable. Pectin-goethite associations may also hinder desorption of $v(PO)$ species at higher organic surface loadings (Table S5). These observations are consistent with the formation of intermolecular organo-organic interactions between glyphosate and pectin functional groups.[16, 51, 54, 55]

The most striking results were found when the $v(CAc)$ bands were deconvoluted across all experiments (Figures 3D-1 to D-4 and S5, S5-2). The stretching and deformation vibrational modes of carboxylate (COO$^-$) and amine (NH$_2^+$) groups, respectively, overlap in the $1700 - 1500$ cm^{-1} range [8, 9, 14]. The carboxylate-amine coupling ($v(CAc)$) can be deconvoluted into four tentative vibrational modes, including two COO$^-$ stretching and two NH$_2^+$ deformation vibrations [8]:

$$v(CAc) = \left(v_{as}\left(\text{COO}^-\right)_I + v_{as}\left(\text{COO}^-\right)_{II} + \delta\left(\text{NH}_2^+\right)_I + \delta\left(\text{NH}_2^+\right)_{II} \right) \qquad \text{(Eq. 3)}$$

Further analysis of deconvoluted spectra was carried out using the summation of vibrational modes of $\delta(\text{NH}_2^+)$ ($\delta(\text{NH}_2^+)_I + \delta(\text{NH}_2^+)_{II}$) and $v_{as}(\text{COO}^-)$ ($v_{as}(\text{COO}^-)_{II} + v_{as}(\text{COO}^-)_{II}$). We found glyphosate's $\delta(\text{NH}_2^+)$ band contribution during the adsorption phase ($X(\delta(\text{NH}_2^+)_{ads}$, S5-1) increased as a function of pectin surface loading, from 28 % on goethite to 45 % on 4 mg mL^{-1} pectin-goethite (Figure 3D-1 to D4, Table S6). Conversely, glyphosate $v_{as}(\text{COO}^-)$ band contribution ($X(v(\text{COO}^-)_{ads})$ diminished with increasing pectin surface loading, from 72 % on

goethite to 55 % on 4 mg mL^{-1} pectin-goethite. The latter may be a result of electrostatic repulsion between surface-associated carboxylates of glyphosate and pectin residues, which is expected to increase with pectin loading at the goethite interface. During desorption, the contribution of $\delta(NH_2^+)$ to $v(CAc)$ bands of retained glyphosate on goethite and on 0.25 mg mL^{-1} pectin-goethite was smaller than during adsorption. However, with increasing surface loading ([Pt] $\geq$ 0.5 mg mL^{-1}), and likely due to the removal of "free" or loosely surface-associated glyphosate species, $X(\delta(NH_2^+))$ increased from 18 % on goethite to 58 % on 4 mg mL^{-1} pectin-goethite during desorption. On the contrary, desorption diminished $X(v(COO^-)_{des}$ contributions, from 82 % on goethite to 42 % on 4 mg mL^{-1} pectin-goethite. Decreased $X(v(COO^-)_{des}$ contributions to $v(CAc)$ bands may relate to the disruption of *OS* glyphosate-pectin complexes from pectin-goethite OMAs. Furthermore, estimated adsorption rate constants (Table S6) indicate surface-associated $\delta(NH_2^+)$ bands of glyphosate evolved faster than corresponding $v_{as}(COO^-)$ bands at higher pectin surface loadings ([Pt] $\geq$ 2.0 mg mL^{-1}). This can be explained by the interfacial electrostatic potential, which is expected to increase for a positive functional group with increasing pectin surface loading due to the increased number of carboxylate functionalities available (pectin used in experiments had an estimated $\approx$ 37% carboxylate content; see S3-1). Interactions between glyphosate-N-H$_2^+$ and pectin-COO$^-$ functionalities are therefore deemed favorable through hydrogen bonding. [16, 37, 56, 57]

Influence of Pectin on Glyphosate Retention: Mechanisms of Interaction

ATR-FTIR spectra show glyphosate interacts with goethite and pectin-goethite interfaces forming distinct surface-associated species during adsorption and desorption experiments (Figure 1B-C, Table S4).[4, 7-9, 12, 14, 19, 20, 50] The phosphonate functional group of glyphosate (1100 – 950

18

cm^{-1}) forms inner-sphere (*IS*) complexes at the goethite interface both in the absence (i.e.,

goethite only) and in the presence of pectin (i.e., pectin-goethite OMAs). Under slightly acidic

conditions, the phosphonate group can form *IS* complexes with goethite, more favorably,

binuclear bidentate without proton (*B*) and mononuclear monodentate with proton (*M-H*) through

ligand-exchange mechanisms.[8, 9, 14] A mononuclear monodentate without proton (*M*) *IS* complex

most likely forms due to the contribution of glyphosate's dianion species.[8, 14] In this study,

surface-associated phosphonate IR bands were centered at approximately 1176 – 1187

($v_{as}(PO_2)_{OS}$), 1140 – 1142 ($v(P=O)$), 1078 – 1082 ($v(PO_2)_{OS} + v(P-O-Fe)_{M-H}$), 1059 – 1061 ($v(P-$

$O-Fe)_{M-H}$), 1013 – 1020 ($v_{as}(P-O-Fe)_B$) and 980 – 987 ($v(PO_3)_{OS} + v_s(P-O-Fe)_B$) cm^{-1} in goethite

adsorption-desorption spectra (Figure 1C, Table S4). In experiments with pectin-goethite

(Figure 1B), surface-associated phosphonate IR bands were centered at approximately 1184 –

1186 ($v_{as}(P-O)_{OS}$), 1160 – 1164 cm^{-1} ($v(PO_2)_{Pt-OS}$), 1132 – 1136 ($v(P=O)$), 1080 – 1091 ($v(PO_2)_{OS}$

$_+ v(P-O-Fe)_{M-H}$), 1061 – 1065 ($v(P-O-Fe)_{M-H}$), 1007 – 1003 ($v_{as}(P-O-Fe)_M$) and 977 – 987

($v(PO_3)_{OS} + v_s(P-O-Fe)_M$) cm^{-1}. The peak at 977 – 987 cm^{-1} is a common symmetrical stretching

vibration mode between *M* and *B* complexes.[8] In contrast, their corresponding asymmetrical

stretching vibration mode at 1005 (*M* complexes) and 1020 (*B* complexes) cm^{-1} were clearly

distinct (Figure 1B-C). At pH = 5.0, the high electrostatic attraction potential at the goethite

surface (pH$_{pzc}$ = 7.3 ± 0.2) increases the energetic favorability to form bidentate complexes

through phosphonate groups. However, the presence of pectin, besides reducing the number of

available surface sites, diminishes this energy thus hindering the formation of bidentate

complexes in favor of monodentate configurations. Hence, glyphosate preferentially forms a *M*

configuration with goethite in pectin-goethite associations whereas a *B* configuration is more

favorable at the goethite interface. Formation of a *M* configuration has been suggested to be

favored at higher pH on the goethite surface.[8, 14] Irrespective of pectin surface loading the peaks at 1059 – 1065 cm^{-1} confirm the formation of a *M-H* complex at the goethite surface across experiments.[9] In contrast to previous work[8], an IR peak for a mononuclear bidentate configuration was not observed in our experiments at pH = 5. A mononuclear bidentate configuration forms a four-membered ring structure which has a relatively unfavorable energy compared with a binuclear bidentate configuration.[7]

Asymmetric and symmetric P-O bands in surface-associated species are influenced by hydrogen bonding. The phosphonate anion is a strong acceptor for hydrogen bridges.[58] In goethite films the uncomplexed v(P=O) band is centered at 1140 cm^{-1} while in pectin-goethite films this band appears at 1132 cm^{-1} (Figure 1B-C, Table S4). This downshift is likely due to intermolecular hydrogen bonding between glyphosate's phosphonate moiety and oxygen- or nitrogen- containing residues in pectin associations. The spectra of pectin-goethite show a shoulder at 1160 – 1164 cm^{-1}: we tentatively assign this feature to a different mode of v_{as}(PO$_2$), i.e., v(PO$_2$)$_{Pt\text{-}OS}$, which is split to lower energies due to hydrogen bonding. Additionally, the upward shift of v_{as}(PO$_2$) from 1181 cm^{-1} in ionic-state (bulk) to $\approx$ 1187 cm^{-1} at the goethite surface at experiment's end ($t_{e,des}$) indicates R-phosphonate dimers were probably lost during adsorption as an *OS* complex.[9, 54] Similar trends were observed for corresponding symmetric stretching bands (Table S4).

The carboxylate and amine groups of glyphosate are thought to contribute to *OS* complexes via weak interactions, such as electrostatic attraction or hydrogen bonding, and strong evidence to imply *IS* complexation through the carboxylate group at the goethite surface is lacking.[8, 9, 14] The v(*CAc*) band of glyphosate (1700 – 1550 cm^{-1}) originates mainly from v_{as}(COO$^-$)$_{II}$ vibrations and its coupling with deformation modes of the NH$_2^+$ group[59] in a zwitterionic structure. Therefore,

time-resolved FTIR analyses of C-O and N-H band shifts can be used to study interactions

between the carboxylate and amine moieties at the goethite and pectin-goethite interfaces. When

compared to corresponding glyphosate vibrations in solution, we observe substantial downward

shifts in the $v_{as}(COO^-)_{II}$ (15 cm^{-1}) and $v_s(COO^-)$ (14 cm^{-1}) vibrational modes at the end of

adsorption-desorption experiments ($t_{e,des}$) at the goethite interface (Table S4). We thus suggest

glyphosate's carboxylate moieties mainly contribute to *OS* complexes via intermolecular

hydrogen bonding that occurs among glyphosate molecules at the goethite surface (e.g.,

glyphosate-C(=O)O$^-$ ···· H$_2$N$^+$-glyphosate and glyphosate-C(=O)O$^-$ ···· HPO$_3$$^{2-}$-glyphosate). This

is in agreement with previous studies where the adsorption modes of carboxylate-containing

organic anions and zwitterions (other than glyphosate) on goethite have been investigated.[20, 59-61]

At the pectin-goethite interface, the observed downward shifts of $v_{as}(COO^-)_{II}$ and $v_s(COO^-)$

vibrational modes (4 and 16 cm^{-1}, respectively) indicate pectin may also induce hydrogen

bonding of uncoordinated carboxylate groups of glyphosate. This asymmetrical downshift for C-

O bands at the pectin-goethite interface might be caused by a different hydrogen bond with

amide residues of pectin (i.e., pectin-N$^+$H$_2$ ···· $^-$O(O=)C-glyphosate). This interaction affects the

positioning of glyphosate molecules within the *OS* region in pectin-goethite OMAs compared to

goethite (Figure 4C-D). The negative progression of interfacial IR signals (Figure 1B) at ≈ 1650

(mainly $v(C=O)$) and ≈ 1549 cm^{-1} (mainly $\delta(N-H)$)[24, 37, 40, 62], tentatively attributed to the loss of

inter- and intra- chain molecular H-bonds in pectin (degree of amidation = 4.14%, section S3-2),

provides further evidence for the formation of new hydrogen bonds between glyphosate and

pectin at pectin-goethite interfaces (Figure 1B, Figure 4D). Along with *IS* complexation of

glyphosate at the goethite surface, these hydrogen bonds could also contribute to the partial

desorption of pectin from goethite (Figure 2) by substitution for interchain hydrogen bonds among pectin residuals.[43]

At experiments' pH of 5, glyphosate NH_2^+ moiety is expected to encounter a repulsive force from the mostly positive-charged goethite surface ($pH_{pzc} = 7.3 \pm 0.2$). As in previous studies of glyphosate adsorption on goethite,[9, 14] we found no evidence for the participation of the NH_2^+ group in surface complexation at the goethite interface. Both interfacial $\delta(NH_2^+)$ vibrations of glyphosate are however shifted to higher energies at the pectin-goethite interface compared to glyphosate in bulk solution (Table S6). These bands also gained intensity relative to interfacial $v_{as}(COO^-)$ bands as a function of pectin surface loading (Figure 3D1-4 and Table S6). These observations imply the presence of pectin alters the extent and type of amine-associated hydrogen bonds present in pectin-goethite OMAs. Hydrogen bonding stabilizes charged resonance structures[63] and the strength of hydrogen bonds can be related to the integrated absorbance of amine bands.[57] Therefore, higher $X(\delta(NH_2^+))$ values and corresponding upshifts with increasing pectin surface loading denote the involvement of the amine moiety through stronger hydrogen bonds with carbonyl-containing functional groups, such as carboxylate and ester residues of pectin (Figure 4D). However, downward shifts of interfacial $\delta(NH_2^+)$ bands on goethite at $t_{e,des}$ occur when intramolecular hydrogen bonding is lost or weakened during glyphosate desorption.[57] This interpretation supports our kinetic data in which the minimum $X(\delta(NH_2^+))$ value was observed at the end of desorption experiments on goethite, and where we suggest amine-meditate interactions were less important.

Overall, this study shows the rate, quantity and mechanisms of glyphosate retention at goethite and pectin-goethite interfaces differ. We first highlight that interfacial retention of glyphosate occurs via phosphonate, carboxylate and amine functionalities. These interactions do not

proportionally contribute to the formation of *IS* and *OS* complexes, but are rather controlled by pectin surface loading (Figure 4A-B). Adsorbed-pectin occupies surface sites on goethite while diminishing the electrostatic attraction of glyphosate for goethite; consequently, the presence of pectin promotes the formation of monodentate rather than bidentate configurations at the goethite interface (Figure 4C-D). Furthermore, we found multiple hydrogen bonds between oxygen- and nitrogen- containing functional groups of pectin and glyphosate facilitate the retention of glyphosate at the pectin-goethite interface (Figure 4D).
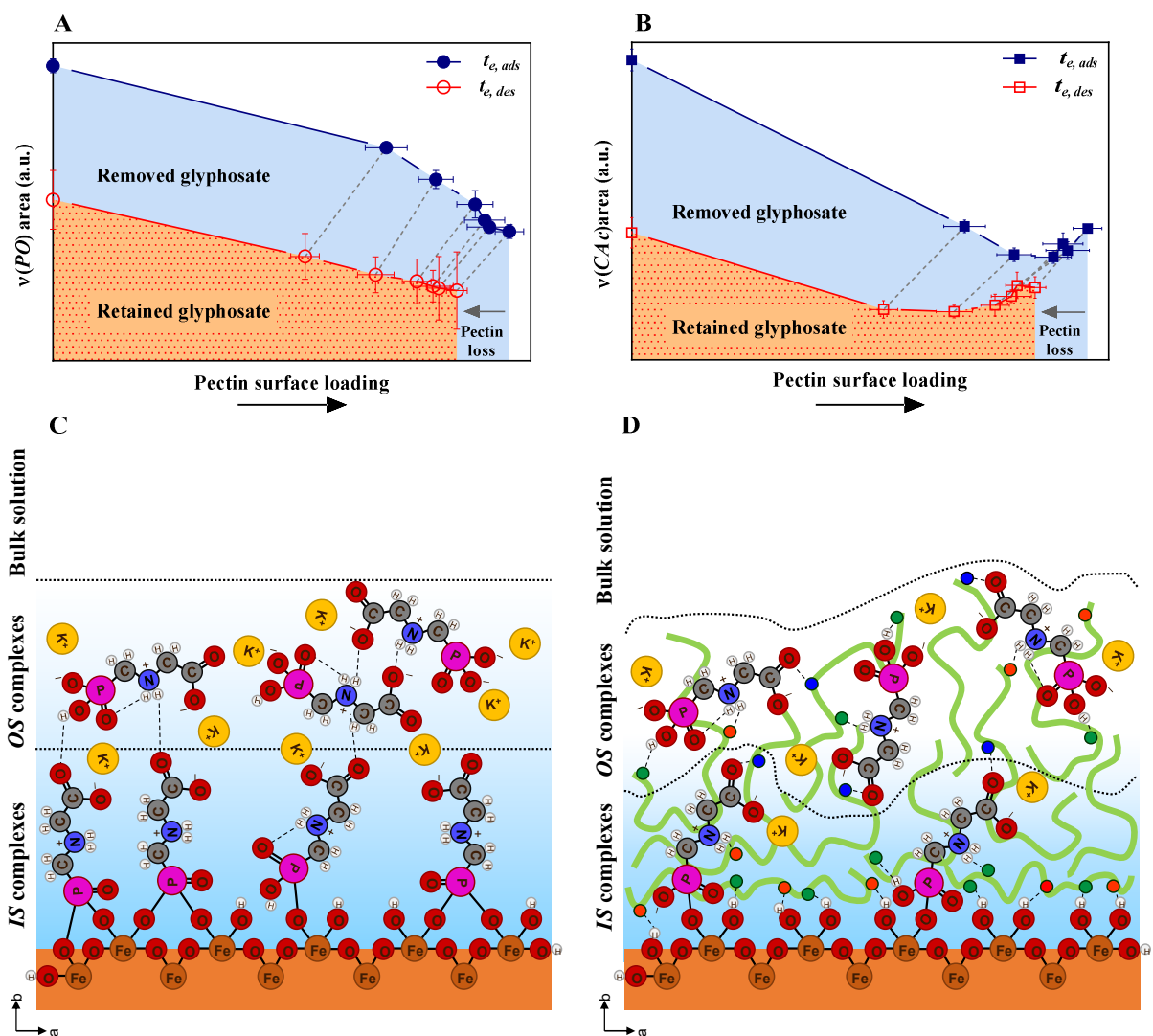
Figure 4. Adsorbed glyphosate at adsorption ($t_{e,ads}$) and desorption ($t_{e,des}$) equilibrium represented by peak areas of the (A) phosphonate ($v(PO)$) and (B) carboxylate-amine ($v(CAc)$) frequency regions in pectin-goethite OMAs with increasing pectin surface loading (i.e., increases in integral $v(CO)(CC)_{ring}$ vibrations). Blue and orange areas in panels (A) and (B) represent the fraction of glyphosate removed and retained at equilibrium, respectively. Conceptualization of glyphosate's interactions at the (C) goethite and (D) pectin-goethite interfaces at $t_{e,des}$. Green wavy lines (D) represent pectin chains and black dashed lines (C and D) represent hydrogen bonds. Blue, green, and red circles (D) represent amide, ester, and carboxylate residues of pectin. For the sake of simplicity, the inter- and intra- chain hydrogen bonds of pectin are not illustrated. *IS*, inner sphere; *OS*, outer sphere.

Environmental Significance

Environmental contamination with glyphosate occurs frequently and widely in U.S. soils, sediments, surface and groundwater.[64-67] In the US alone, the application rate of glyphosate was estimated at $\approx 107 \times 10^6$ kg year^{-1} (2012-2019), with more than 74% applied to agricultural crops (soybean, corn, cotton and sunflower).[68, 69] Molecular-scale studies of glyphosate retention dynamics at organo-mineral interfaces, as presented in this work, are relevant since surface soils contain minerals that are mostly, if not completely, coated with organic molecules. While glyphosate's environmental fate is strongly influenced by organo-mineral associations, research in this area is still inadequate and results unclear, which currently represents a considerable knowledge gap.[8, 12, 16]

This work demonstrates how an organo-mineral association (i.e., pectin-goethite) modulates the extent, kinetics and mechanisms of interaction of glyphosate. Mechanistically, we found the

presence of pectin alters the proportion and type of interactions glyphosate undertakes at the pectin-goethite compared to the goethite interface (Figure 4C-D). Although inner-sphere complexes dominate in phosphonate-associated species, the presence of pectin results in the successive disappearance of the bidentate configuration on goethite while promoting the formation of monodentate configurations on goethite at pectin-goethite interfaces. To our knowledge, this is the first study that demonstrates the contribution of carboxylate and amine functional groups of glyphosate to outer-sphere species on goethite and pectin-goethite associations through intermolecular hydrogen bonds. Hydrogen bonds between the carboxylate and amine functionalities of glyphosate and the oxygen- and nitrogen- containing functional groups of adsorbed pectin impacts glyphosate's retention capacity and adsorption-desorption rates. The extent to which glyphosate was retained at pectin-goethite interfaces was reduced compared to that at the goethite interface, with reduced retention at higher pectin surface loadings (Figure 4A-B). Notably, the retention of amine-associated glyphosate species increased relative to interfacial carboxylate-associated species as a function of pectin surface loading. We attribute this shift to the formation of hydrogen bonds between the amine group of glyphosate and the carboxylate residues of pectin (Figure 4D). We suggest these hydrogen bond interactions slowed the desorption of glyphosate from pectin-goethite interfaces with increasing surface loading. More generally, increased pectin loading in pectin-goethite associations results in slower glyphosate retention processes (i.e., adsorption-desorption kinetics) compared to corresponding processes at the goethite interface. However, carboxylate- and amine-associated glyphosate species had faster adsorption kinetics than phosphonate-associated species, which may be linked to the formation of outer- and inner- sphere complexes (respectively), with faster kinetics for the formation of outer-sphere complexes in pectin-goethite and to reduced

accessibility of glyphosate molecules for active sites on goethite. Once formed, carboxylate- and amine-associated species desorbed more slowly than phosphonate-associated species.

Overall, our molecular-scale studies highlight the impact of natural organic matter (e.g., pectin) on glyphosate's mobility at heterogeneous interfaces present in soils. In addition, since the proportion of organo-mineral interfaces to mineral interfaces decreases with soil depth, our work provides insights as to the extent, kinetics and mechanisms that might be involved during glyphosate downward transport. Ultimately, this knowledge could lead to better predictions of glyphosate occurrence in natural systems and risk assessments.

Acknowledgments

Supporting Information

Detailed descriptions of goethite synthesis, preparation of pectin-goethite thin films for *in-situ* ATR-FTIR experiments, pectin characterization, adsorption-desorption kinetic models, adsorbed pectin, glyphosate peak assignments, and deconvolution and peak fitting analysis.

Corresponding Author

Carmen Enid Martínez - Soil and Crop Sciences, School of Integrative Plant Science, College of Agriculture and Life Sciences, Cornell University, Ithaca, New York 14853, USA; http://orcid.org/0000-0001-8553-2118; Email: cem20@cornell.edu

Author

Behrooz Azimzadeh - Soil and Crop Sciences, School of Integrative Plant Science, College of Agriculture and Life Sciences, Cornell University, Ithaca, New York 14853, USA; https://orcid.org/0000-0001-9497-9843; Email: ba324@cornell.edu

Notes

The authors declare no competing financial interests.

References

1. Nadin, P. The use of plant protection products in the European union data 1992–2003. *European Commission: Luxembourg, France* **2007**.
2. Li, H.; Wallace, A. F.; Sun, M.; Reardon, P.; Jaisi, D. P. Degradation of glyphosate by Mn-oxide may bypass sarcosine and form glycine directly after C–N bond cleavage. *Environmental science & technology* **2018,** *52* (3), 1109-1117.
3. Huhn, C. More and enhanced glyphosate analysis is needed. *Analytical and bioanalytical chemistry* **2018,** *410* (13), 3041-3045.
4. Undabeytia, T.; Morillo, E.; Maqueda, C. FTIR Study of Glyphosate−Copper Complexes. *Journal of Agricultural and Food Chemistry* **2002,** *50* (7), 1918-1921.

5. Subramaniam, V.; Hoggard, P. E. Metal complexes of glyphosate. *Journal of agricultural and food chemistry* **1988,** *36* (6), 1326-1329.
6. Sheals, J.; Persson, P.; Hedman, B. IR and EXAFS Spectroscopic Studies of Glyphosate Protonation and Copper(II) Complexes of Glyphosate in Aqueous Solution. *Inorganic Chemistry* **2001,** *40* (17), 4302-4309.
7. Barja, B. C.; dos Santos Afonso, M. An ATR−FTIR Study of Glyphosate and Its Fe(III) Complex in Aqueous Solution. *Environmental Science & Technology* **1998,** *32* (21), 3331-3335.
8. Yan, W.; Jing, C. Molecular Insights into Glyphosate Adsorption to Goethite Gained from ATR-FTIR, Two-Dimensional Correlation Spectroscopy, and DFT Study. *Environmental science & technology* **2018,** *52* (4), 1946-1953.
9. Sheals, J.; Sjöberg, S.; Persson, P. Adsorption of glyphosate on goethite: molecular characterization of surface complexes. *Environmental science & technology* **2002,** *36* (14), 3090-3095.
10. Elzinga, E. J.; Sparks, D. L. Phosphate adsorption onto hematite: An in situ ATR-FTIR investigation of the effects of pH and loading level on the mode of phosphate surface complexation. *Journal of Colloid and Interface Science* **2007,** *308* (1), 53-70.
11. Albers, C. N.; Banta, G. T.; Hansen, P. E.; Jacobsen, O. S. The influence of organic matter on sorption and fate of glyphosate in soil–Comparing different soils and humic substances. *Environmental pollution* **2009,** *157* (10), 2865-2870.
12. Arroyave, J. M.; Waiman, C. C.; Zanini, G. P.; Avena, M. J. Effect of humic acid on the adsorption/desorption behavior of glyphosate on goethite. Isotherms and kinetics. *Chemosphere* **2016,** *145*, 34-41.
13. Barrett, K. A.; McBride, M. B. Oxidative Degradation of Glyphosate and Aminomethylphosphonate by Manganese Oxide. *Environmental Science & Technology* **2005,** *39* (23), 9223-9228.
14. Barja, B. C.; dos Santos Afonso, M. Aminomethylphosphonic Acid and Glyphosate Adsorption onto Goethite: A Comparative Study. *Environmental Science & Technology* **2005,** *39* (2), 585-592.
15. Glass, R. L. Adsorption of glyphosate by soils and clay minerals. *Journal of Agricultural and Food Chemistry* **1987,** *35* (4), 497-500.
16. Guo, F.; Zhou, M.; Xu, J.; Fein, J. B.; Yu, Q.; Wang, Y.; Huang, Q.; Rong, X. Glyphosate adsorption onto kaolinite and kaolinite-humic acid composites: Experimental and molecular dynamics studies. *Chemosphere* **2021,** *263*, 127979.
17. McBride, M.; Kung, K.-H. Complexation of Glyphosate and Related Ligands with Iron (III). *Soil Science Society of America Journal* **1989,** *53* (6), 1668-1673.
18. Tribe, L.; Kwon, K. D.; Trout, C. C.; Kubicki, J. D. Molecular orbital theory study on surface complex structures of glyphosate on goethite: calculation of vibrational frequencies. *Environmental science & technology* **2006,** *40* (12), 3836-3841.
19. Waiman, C. V.; Avena, M. J.; Regazzoni, A. E.; Zanini, G. P. A real time in situ ATR-FTIR spectroscopic study of glyphosate desorption from goethite as induced by phosphate adsorption: Effect of surface coverage. *Journal of Colloid and Interface Science* **2013,** *394*, 485-489.
20. Yang, Y.; Wang, S.; Xu, Y.; Zheng, B.; Liu, J. Molecular-Scale Study of Aspartate Adsorption on Goethite and Competition with Phosphate. *Environmental Science & Technology* **2016,** *50* (6), 2938-2945.

21. Kögel-Knabner, I. The macromolecular organic composition of plant and microbial residues as inputs to soil organic matter. *Soil Biology and Biochemistry* **2002,** *34* (2), 139-162.

22. Manucharova, N. The microbial destruction of chitin, pectin, and cellulose in soils. *Eurasian Soil Science* **2009,** *42* (13), 1526-1532.

23. Mohnen, D. Pectin structure and biosynthesis. *Current Opinion in Plant Biology* **2008,** *11* (3), 266-277.

24. Chatjigakis, A. K.; Pappas, C.; N.Proxenia; O.Kalantzi; P.Rodis; Polissiou, M. FT-IR spectroscopic determination of the degree of esterification of cell wall pectins from stored peaches and correlation to textural changes. *Carbohydrate Polymers* **1998,** *37* (4), 395-408.

25. Schmidt, M. P.; Martínez, C. E. Supramolecular association impacts biomolecule adsorption onto goethite. *Environmental science & technology* **2018,** *52* (7), 4079-4089.

26. Schmidt, M. P.; Siciliano, S. D.; Peak, D. Spectroscopic Quantification of Inner- and Outer-Sphere Oxyanion Complexation Kinetics: Ionic Strength and Background Cation Effect on Sulfate Adsorption to Hematite. *ACS Earth and Space Chemistry* **2020,** *4* (10), 1765-1776.

27. Hettiarachchi, C. A.; Melton, L. D.; Williams, M. A.; McGillivray, D. J.; Gerrard, J. A.; Loveday, S. M. M orphology of complexes formed between β-lactoglobulin nanofibrils and pectins is influenced by the pH and structural characteristics of the pectins. *Biopolymers* **2016,** *105* (11), 819-831.

28. Yapo, B. M. Rhamnogalacturonan-I: a structurally puzzling and functionally versatile polysaccharide from plant cell walls and mucilages. *Polymer Reviews* **2011,** *51* (4), 391-413.

29. Méndez, D. A.; Fabra, M. J.; Gómez-Mascaraque, L.; López-Rubio, A.; Martinez-Abad, A. Modelling the Extraction of Pectin towards the Valorisation of Watermelon Rind Waste. *Foods* **2021,** *10* (4), 738.

30. Rockwell, P. L.; Kiechel, M. A.; Atchison, J. S.; Toth, L. J.; Schauer, C. L. Various-sourced pectin and polyethylene oxide electrospun fibers. *Carbohydrate Polymers* **2014,** *107*, 110-118.

31. Schwertmann, U.; Cornell, R. M., *Iron oxides in the laboratory: preparation and characterization*. John Wiley & Sons: 2008.

32. Sakurai, K.; Ohdate, Y.; Kyuma, K. Comparison of salt titration and potentiometric titration methods for the determination of Zero Point of Charge (ZPC). *Soil Science and Plant Nutrition* **1988,** *34* (2), 171-182.

33. Tan, W.-f.; Lu, S.-j.; Liu, F.; Feng, X.-h.; He, J.-z.; Koopal, L. K. DETERMINATION OF THE POINT-OF-ZERO CHARGE OF MANGANESE OXIDES WITH DIFFERENT METHODS INCLUDING AN IMPROVED SALT TITRATION METHOD. *Soil Science* **2008,** *173* (4).

34. Lagergren, S. Zur theorie der sogenannten adsorption geloster stoffe. **1898**.

35. Synytsya, A.; Čopíková, J.; Matějka, P.; Machovič, V. Fourier transform Raman and infrared spectroscopy of pectins. *Carbohydrate Polymers* **2003,** *54* (1), 97-106.

36. Šimkovic, I.; Synytsya, A.; Uhliariková, I.; Čopíková, J. Amidated pectin derivatives with n-propyl-, 3-aminopropyl-, 3-propanol- or 7-aminoheptyl-substituents. *Carbohydrate Polymers* **2009,** *76* (4), 602-606.

37. Sinitsya, A.; Čopíková, J.; Prutyanov, V.; Skoblya, S.; Machovič, V. Amidation of highly methoxylated citrus pectin with primary amines. *Carbohydrate Polymers* **2000,** *42* (4), 359-368.

38. Meneguzzo, F.; Brunetti, C.; Fidalgo, A.; Ciriminna, R.; Delisi, R.; Albanese, L.; Zabini, F.; Gori, A.; dos Santos Nascimento, L. B.; De Carlo, A.; Ferrini, F.; Ilharco, L. M.; Pagliaro,

M. Real-Scale Integral Valorization of Waste Orange Peel via Hydrodynamic Cavitation. *Processes* **2019,** *7* (9), 581.
39. Fidalgo, A.; Ciriminna, R.; Carnaroglio, D.; Tamburino, A.; Cravotto, G.; Grillo, G.; Ilharco, L. M.; Pagliaro, M. Eco-Friendly Extraction of Pectin and Essential Oils from Orange and Lemon Peels. *ACS Sustainable Chemistry & Engineering* **2016,** *4* (4), 2243-2251.
40. Assifaoui, A.; Loupiac, C.; Chambin, O.; Cayot, P. Structure of calcium and zinc pectinate films investigated by FTIR spectroscopy. *Carbohydrate Research* **2010,** *345* (7), 929-933.
41. Canteri, M. H. G.; Renard, C. M. G. C.; Le Bourvellec, C.; Bureau, S. ATR-FTIR spectroscopy to determine cell wall composition: Application on a large diversity of fruits and vegetables. *Carbohydrate Polymers* **2019,** *212*, 186-196.
42. Guzman-Puyol, S.; Benítez, J. J.; Domínguez, E.; Bayer, I. S.; Cingolani, R.; Athanassiou, A.; Heredia, A.; Heredia-Guerrero, J. A. Pectin-Lipid Self-Assembly: Influence on the Formation of Polyhydroxy Fatty Acids Nanoparticles. *PLOS ONE* **2015,** *10* (4), e0124639.
43. Azimzadeh, B.; Martinez, C. E. Multiple interchain hydrogen-bonding interactions of pectin at water-mineral interfaces revealed by ATR-FTIR spectroscopy. *Colloids and Surfaces A: Physicochemical and Engineering Aspects* **2022,** *XX* (XXX).
44. Schmidt, M. P.; Martínez, C. E. Kinetic and Conformational Insights of Protein Adsorption onto Montmorillonite Revealed Using in Situ ATR-FTIR/2D-COS. *Langmuir* **2016,** *32* (31), 7719-7729.
45. Schmidt, M. P.; Martínez, C. E. Ironing Out Genes in the Environment: An Experimental Study of the DNA–Goethite Interface. *Langmuir* **2017,** *33* (34), 8525-8532.
46. Keiluweit, M.; Bougoure, J. J.; Nico, P. S.; Pett-Ridge, J.; Weber, P. K.; Kleber, M. Mineral protection of soil carbon counteracted by root exudates. *Nature Climate Change* **2015,** *5* (6), 588-595.
47. Yuan, Y.; Zhang, Z.; Chen, L.; Yang, Z.; Liu, J. Facilitated destabilization of physicochemically protected soil organic matter by root-derived low-molecular-weight organic acids. *Journal of Soils and Sediments* **2022,** *22* (6), 1677-1686.
48. Li, W.; Wang, Y.-J.; Zhu, M.; Fan, T.-T.; Zhou, D.-M.; Phillips, B. L.; Sparks, D. L. Inhibition Mechanisms of Zn Precipitation on Aluminum Oxide by Glyphosate: A 31P NMR and Zn EXAFS Study. *Environmental Science & Technology* **2013,** *47* (9), 4211-4219.
49. Chen, Z.; He, W.; Beer, M.; Megharaj, M.; Naidu, R. Speciation of glyphosate, phosphate and aminomethylphosphonic acid in soil extracts by ion chromatography with inductively coupled plasma mass spectrometry with an octopole reaction system. *Talanta* **2009,** *78* (3), 852-856.
50. Zenobi, M. C.; Luengo, C. V.; Avena, M. J.; Rueda, E. H. An ATR-FTIR study of different phosphonic acids in aqueous solution. *Spectrochimica Acta Part A: Molecular and Biomolecular Spectroscopy* **2008,** *70* (2), 270-276.
51. Miano, T.; Piccolo, A.; Celano, G.; Senesi, N. Infrared and fluorescence spectroscopy of glyphosate-humic acid complexes. *Science of the total environment* **1992,** *123*, 83-92.
52. Waiman, C. V.; Arroyave, J. M.; Chen, H.; Tan, W.; Avena, M. J.; Zanini, G. P. The simultaneous presence of glyphosate and phosphate at the goethite surface as seen by XPS, ATR-FTIR and competitive adsorption isotherms. *Colloids and Surfaces A: Physicochemical and Engineering Aspects* **2016,** *498*, 121-127.
53. Young, A. G.; McQuillan, A. J. Adsorption/Desorption Kinetics from ATR-IR Spectroscopy. Aqueous Oxalic Acid on Anatase TiO2. *Langmuir* **2009,** *25* (6), 3538-3548.

54. Piccolo, A.; Celano, G. Hydrogen-bonding interactions between the herbicide glyphosate and water-soluble humic substances. *Environmental Toxicology and Chemistry: An International Journal* **1994,** *13* (11), 1737-1741.

55. Mazzei, P.; Piccolo, A. Quantitative evaluation of noncovalent interactions between glyphosate and dissolved humic substances by NMR spectroscopy. *Environmental science & technology* **2012,** *46* (11), 5939-5946.

56. Gu, Z.; Zambrano, R.; McDermott, A. Hydrogen Bonding of Carboxyl Groups in Solid-State Amino Acids and Peptides: Comparison of Carbon Chemical Shielding, Infrared Frequencies, and Structures. *Journal of the American Chemical Society* **1994,** *116* (14), 6368-6372.

57. Wang, F. C.; Feve, M.; Lam, T. M.; Pascault, J.-P. FTIR analysis of hydrogen bonding in amorphous linear aromatic polyurethanes. I. Influence of temperature. *Journal of Polymer Science Part B: Polymer Physics* **1994,** *32* (8), 1305-1313.

58. Pohle, W.; Bohl, M.; Böhlig, H. Interpretation of the influence of hydrogen bonding on the stretching vibrations of the PO^-2 moiety. *Journal of Molecular Structure* **1991,** *242*, 333-342.

59. Norén, K.; Loring, J. S.; Persson, P. Adsorption of alpha amino acids at the water/goethite interface. *Journal of Colloid and Interface Science* **2008,** *319* (2), 416-428.

60. Liang, J.; Horton, J. H. Interactions of Benzoic Acid and Phosphates with Iron Oxide Colloids Using Chemical Force Titration. *Langmuir* **2005,** *21* (23), 10608-10614.

61. Norén, K.; Persson, P. Adsorption of monocarboxylates at the water/goethite interface: The importance of hydrogen bonding. *Geochimica et Cosmochimica Acta* **2007,** *71* (23), 5717-5730.

62. Barth, A. Infrared spectroscopy of proteins. *Biochimica et Biophysica Acta (BBA) - Bioenergetics* **2007,** *1767* (9), 1073-1101.

63. Myshakina, N. S.; Ahmed, Z.; Asher, S. A. Dependence of Amide Vibrations on Hydrogen Bonding. *The Journal of Physical Chemistry B* **2008,** *112* (38), 11873-11877.

64. Battaglin, W. A.; Meyer, M. T.; Kuivila, K. M.; Dietze, J. E. Glyphosate and its degradation product AMPA occur frequently and widely in US soils, surface water, groundwater, and precipitation. *JAWRA Journal of the American Water Resources Association* **2014,** *50* (2), 275-290.

65. Kolpin, D. W.; Thurman, E. M.; Lee, E. A.; Meyer, M. T.; Furlong, E. T.; Glassmeyer, S. T. Urban contributions of glyphosate and its degradate AMPA to streams in the United States. *Science of The Total Environment* **2006,** *354* (2), 191-197.

66. Battaglin, W. A.; Kolpin, D. W.; Scribner, E. A.; Kuivila, K. M.; Sandstrom, M. W. Glyphosate, other herbicides, and transformation products in midwestern streams, 20021. *JAWRA Journal of the American Water Resources Association* **2005,** *41* (2), 323-332.

67. Skark, C.; Zullei-Seibert, N.; Schöttler, U.; Schlett, C. The occurrence of glyphosate in surface water. *International Journal of Environmental Analytical Chemistry* **1998,** *70* (1-4), 93-104.

68. Wieben, C. *Estimated annual agricultural pesticide use by major crop or crop group for states of the conterminous United States, 1992-2019 (including preliminary estimates for 2018-19): U.S. Geological Survey data release*; 2021.

69. Hawkins, C.; Hanson, C. *Glyphosate: Response to Comments, Usage, and Benefits (PC Codes: 103601, 103604, 103605, 103607, 103608, 103613, 417300)*; Environmental Protection Agency: 2019.